The Journal of Chemical Physics

Glass polyamorphism in gallium: Two amorphous solid states and their transformation on the potential energy landscape

Cite as: J. Chem. Phys. **154**, 134503 (2021); https://doi.org/10.1063/5.0038058
Submitted: 18 November 2020 . Accepted: 11 February 2021 . Published Online: 01 April 2021

Yizhi Liu, Gang Sun, and Limei Xu

AIP Publishing

The Journal of Chemical Physics ARTICLE scitation.org/journal/jcp

Glass polyamorphism in gallium: Two amorphous solid states and their transformation on the potential energy landscape

Cite as: J. Chem. Phys. 154, 134503 (2021); doi: 10.1063/5.0038058
Submitted: 18 November 2020 • Accepted: 11 February 2021 •
Published Online: 1 April 2021

Yizhi Liu,[1] Gang Sun,[2,a)] and Limei Xu[1,3,4,a)]

AFFILIATIONS

[1]International Center for Quantum Materials, School of Physics, Peking University, Beijing 100871, China
[2]School of Chemistry, University of Sydney, Sydney, New South Wales, Australia
[3]Collaborative Innovation Center of Quantum Matter, Beijing, China
[4]Interdisciplinary Institute of Light-Element Quantum Materials and Research Center for Light-Element Advanced Materials, Peking University, Beijing 100871, China

Note: This paper is part of the JCP Special Collection in Honor of Women in Chemical Physics and Physical Chemistry.
[a)]**Authors to whom correspondence should be addressed:** gangsun@sydney.edu.au and limei.xu@pku.edu.cn

ABSTRACT

Using the potential energy landscape (PEL) formalism and molecular dynamics simulations, we investigate a phase transformation between two amorphous solid states of gallium, namely, a low-density amorphous solid (LDA) and a high-density amorphous solid (HDA), and compare with its equilibrium counterpart, the liquid–liquid phase transition (LLPT). It is found that on the PEL, the signatures of the out-of-equilibrium LDA–HDA transition are reminiscent of those of the equilibrium LLPT in terms of pressure, inherent structure pressure, inherent structure energy, and shape function, indicating that the LDA–HDA transformation is a first-order-like transition. However, differences are also found between the out-of-equilibrium phase transition and the equilibrium one, for example, the path from LDA to HDA on the PEL cannot be accessed by the path from LDL to HDL. Our results also suggest that the signatures of the out-of-equilibrium transition in gallium are rather general features of systems with an accessible LLPT—not only systems with pairwise interactions but also those with many-body interactions. This finding is of crucial importance for obtaining a deeper understanding of the nature of transitions in the polyamorphic family.

I. INTRODUCTION

A variety of materials with component elements from Groups I, III, and IV of the Periodic Table and from the transition metals, for example, water,[1–3] silicon,[4] and cerium,[5] exhibit anomalies in certain properties such as density and diffusivity. Several explanations of these anomalies have been proposed, among which the liquid–liquid phase transition (LLPT) scenario is widely accepted, particularly in the case of water,[6–14] phosphorus,[15] silicon,[4,16–20] and silica.[21] However, the existence of LLPTs remains controversial,[22–26] since direct detection of an LLPT or its terminal point, namely, the liquid–liquid critical point (LLCP), is difficult owing to unavoidable crystallization in the deeply supercooled regime. According to the LLCP scenario, cooling a low-density liquid (LDL) and a high-density liquid (HDL) will lead to a low-density amorphous (LDA) solid and a high-density amorphous (HDA) solid, respectively. In the 1980s, Mishima *et al.*[27,28] reported a first-order-like transition from LDA ice to HDA ice upon compression, opening up the possibility of investigating LLPTs from the nonequilibrium phase region. That is, the LDA–HDA transformation in the nonequilibrium phase region, if extended into the liquid states, would become an LDL–HDL phase transition. It is commonly believed that the behavior of the glass and liquid states is essentially related.[6,22,23] In a recent experimental study,[29] HDA ice has been used to deduce the existence of an LLPT in water. In the past two decades, many studies[30–45] have been performed to explore the relation between equilibrium/nonequilibrium states (LDL/LDA and HDL/HDA) and their transformations. Most of these studies have focused on water or

water-like model systems with pairwise interactions, such as the ST2 model,[30] the simple point charge extended (SPC/E) model,[31] the Jagla model,[34] and the Fermi–Jagla model,[35,45] but there has been a lack of investigations of systems involving many-body interactions, particularly metallic systems with contributions from itinerant electrons.

Gallium is an intriguing material with complex properties.[46–48] Using the modified embedded-atom model (MEAM),[49,50] Jara *et al.*[51] reported that gallium has two liquid states and exhibits a first-order LLPT. Li *et al.*[48] reported that gallium exhibits numerous water-like anomalies, including density and diffusivity anomalies. The many-body nature of the MEAM potential requires that the interaction between gallium particles depends not only on the distances between two atoms but also on their local charge densities. Therefore, it is a good example for investigating the relation between an out-of-equilibrium state and its equilibrium counterpart, as well as the corresponding phase transformations in polyamorphic systems with many-body interactions. Moreover, if the corresponding amorphous solid transition could be found in gallium, it would provide important information for the experimental search for LLPTs based on out-of-equilibrium phase transitions in metallic systems and is also important for further understanding of the nature of polyamorphism in general.

Currently, characterization of phase transitions between out-of-equilibrium (amorphous solid) states, such as the LDA–HDA transition, remains challenging since it requires answers to some fundamental questions of statistical mechanics, such as how one can properly define or interpret a "phase transition" between out-of-equilibrium glassy states. This question has recently been addressed in some model systems, such as the ST2 model for water and the Fermi–Jagla model[30,35] with pairwise interactions, using the potential energy landscape (PEL) formalism. However, it is not evident how general the conclusions of Refs. 30 and 35 are. In particular, these models involve only pairwise interactions, and the effects of many-body interactions are not yet known, which also makes gallium an especially important candidate to explore.

In this work, we explore the signatures of the LDA–HDA transformation in gallium using the PEL formalism[52–54] and assess the nature of this transformation, such as whether it is a first-order-like phase transition, by comparing it with its equilibrium counterpart, the LLPT. Our results show that two out-of-equilibrium amorphous solid states (LDA and HDA), found at low temperatures, can transform into each other upon compression/decompression. In the PEL, the LDA–HDA transformation of gallium at low temperatures shares certain key features (e.g., a negative curvature in the inherent energy) with the LLPT, suggesting that the LDA–HDA transformation is a first-order-like phase transition. It is also found that the path from LDA to HDA on the energy surface is different from that of the LLPT. This study shows that the PEL formalism, a theoretical framework within statistical mechanics, could provide very useful information on the supercooled liquid and glassy states of metallic systems.

The remainder of this paper is organized as follows: In Sec. II, we present the details of the computer simulations and the method of analysis. The results are given in Sec. III, where we discuss the glass–glass transformation and compare it with the LLPT. A summary is given in Sec. IV.

II. COMPUTER SIMULATIONS AND METHOD OF ANALYSIS

Our system consists of 1152 particles. Each gallium atom has a molar mass of 69.72 g/mol. The interaction between gallium particles in our system is described by the MEAM,[49,50] which is fitted predominantly to results from density functional theory (DFT) calculations with parameters determined by generalized gradient approximation (GGA) calculations.[55] Both constant volume and temperature (*NVT*) and constant pressure and temperature (*NPT*) ensembles are applied to equilibrium states during the compression and decompression processes. Temperature T and pressure P are controlled by the Nosé–Hoover algorithm. Periodic boundary conditions are employed in all the simulations.

Molecular dynamics (MD) simulations with the LAMMPS package[56] are performed to study the PEL in configuration space, which is used to investigate the amorphous–amorphous transformation and LLPT of gallium. To calculate the PEL properties of the system, for liquids at a given (T, V), extensive MD simulations are performed to obtain independent inherent structures (ISs; see below). At each state point, 100 independent configurations are extracted from the MD simulations. We use two approaches to extract the 100 independent configurations: (1) for $T > 400$ K, we extract 100 independent configurations by selecting configurations spaced out in time; (2) for $T \leq 400$ K, the 100 configurations are collected from 100 independent simulations. The ISs are obtained from these 100 configurations by energy minimization using the conjugate gradient algorithm. For amorphous solid states, during the compression and decompression runs, configurations are saved every 400 MPa to obtain the ISs with a compression rate of 10 MPa/ns.

The PEL is a statistical mechanical approach that formally separates the configurational contributions to the partition function into contributions from local energy minima (the IS) and vibrational excitations within the basins of attraction surrounding these minima. For a system consisting of N particles, PEL is an energy surface in $(3N + 1)$-dimensional space as a function of the atom coordinates: $V(\vec{r}_1, \vec{r}_2, \ldots, \vec{r}_n)$.[52] At a given time t, the system is represented by a single point on the PEL given by the coordinates of all atoms at t. Hence, as the system evolves with time, the representative point moves along a trajectory on the PEL.[30,35,53,57] At high temperatures, the representative point can travel over a large region of the PEL, while at low temperatures, it is constrained to move within more localized regions of the PEL. The PEL is composed of large basins, and it is the local minima in these basins that are usually referred to as "inherent structures" (ISs). Based on the harmonic approximation and topography of the PEL, a complete theory has been developed that allows us to express the free energy of liquids in terms of the IS potential energy E_{IS} (local minima of the PEL), the frequency of vibrations (curvature or shape function) in ISs, and the distribution of ISs on the PEL.[52–54,58] As a well-established approach in nonequilibrium physics, the PEL is a useful tool for studying supercooled liquids and glasses at low temperatures.

The evolution of structure in configuration space can be described by three quantities in the PEL method: the IS pressure P_{IS}, the IS energy E_{IS}, and the shape function S_{IS}. The virial expression for the pressure of the IS configuration defines P_{IS}.[59] The curvature of a basin near the energy minimum (the IS) is quantified by the

shape function S_{IS}, which is defined as

$$S_{IS} = \frac{1}{N}\sum_{i=1}^{3N} \ln\left(\frac{\omega_i}{\omega_o}\right), \quad (1)$$

where ω_i (i = 1, 2, ..., $3N$) is from the set of eigenvalues ω_i^2 of the Hessian matrix evaluated at the IS configuration. The constant ω_0 makes the logarithm function dimensionless (here, ω_0 = 1.0 THz). The three fundamental properties of the PEL (P_{IS}, E_{IS}, and S_{IS}) sampled by the system during the LLPT and the compression-induced LDA-to-HDA transformation allow us to characterize the PEL basins associated with these states.

The thermodynamics of an equilibrium LLPT can be analyzed from the behaviors of P_{IS}, E_{IS}, and S_{IS} in the PEL formalism as follows.[35,37,53] According to the second law of thermodynamics, a system is stable only if $\partial^2 F/\partial V^2 > 0$, where F is the free energy in the NVT ensemble. In the PEL formalism, the free energy F of the system can be divided into two parts: $F = F_{IS} + F_{vib}$, where F_{IS} is the contribution from the IS and F_{vib} is the contribution from thermal vibrations. Accordingly, stability requires

$$\frac{\partial^2 F_{IS}}{\partial V^2} + \frac{\partial^2 F_{vib}}{\partial V^2} > 0. \quad (2)$$

Since $P = -\partial F/\partial V$, the pressure can also be divided into two parts: $P = P_{IS} + P_{vib}$, where P_{IS} is the contribution from the IS and P_{vib} is the contribution from thermal vibrations. The stability criterion becomes

$$-\frac{\partial P_{IS}}{\partial V} - \frac{\partial P_{vib}}{\partial V} > 0. \quad (3)$$

In the harmonic approximation, P_{vib} can be expressed as $P_{vib} = -Nk_BT(\partial S_{IS}/\partial V)_{e_{IS},N}$. We then have

$$-\frac{\partial P_{IS}}{\partial V} + Nk_BT\left(\frac{\partial^2 S_{IS}}{\partial V^2}\right)_{e_{IS},N} > 0. \quad (4)$$

A phase transition occurs if $-\partial P_{IS}/\partial V < 0$ and $(\partial^2 S_{IS}/\partial V^2)_{e_{IS},N} < 0$, or at least one of them is negative. Since $P_{IS} = -\partial e_{IS}/\partial V$, the stability criterion becomes

$$\frac{\partial^2 e_{IS}}{\partial V^2} + Nk_BT\left(\frac{\partial^2 S_{IS}}{\partial V^2}\right)_{e_{IS},N} > 0. \quad (5)$$

A first-order phase transition occurs when $\partial^2 e_{IS}/\partial V^2 < 0$ and $(\partial^2 S_{IS}/\partial V^2)_{e_{IS},N} < 0$, or at least one of the curvatures of e_{IS} and S_{IS} is negative, where the former is equivalent to a positive slope of $P_{IS}(v)$ in thermodynamics.

III. RESULTS

A. LDA and HDA states and their transformation

Previous simulation studies[48,51] showed that gallium has two liquid states, namely, a low-density state (LDL) and a high-density state (HDL), separated by a first-order phase transition line (LLPT) ending at an LLCP estimated to be located at T_c = 447.5 K and P_c = 2.18 GPa.[51]

Here, the low-density glassy state (LDA) of gallium is obtained by cooling LDL samples from T = 420 K to 200 K along P = −1.80 GPa at a rate q_c = 0.25 K/ns, while the high-density glassy state (HDA) is obtained by cooling HDL samples from T = 400 K to 200 K along P = 5.40 GPa at a rate q_c = 0.4 K/ns. The LDA produced by rapid cooling is also called hyperquenched glassy gallium (HGG). The radial distribution functions (RDFs) for LDA and HDA are shown in Figs. 1(a) and 1(b), respectively. As can be seen, the frozen amorphous glasses have similar structures to their parent liquids. We calculate the number of nearest neighbors in the two liquids by integrating the RDF $g(r)$ from r = 0 to r_{min} chosen as the distance of the first minimum of $g(r)$. This number is 8 for LDA and 9 for HDA.[48] It is found that in terms of local packing, HDA differs from LDA mainly in the distribution of the ninth-nearest-neighbors [see the insets in Figs. 1(a) and 1(b)].

The HDA and LDA can also be obtained through isothermal compression of LDA and decompression of HDA, respectively.[27,28] For instance, by taking an LDA configuration formed at P = −1.8 GPa and compressing it to P = 8.15 GPa along T = 200 K, a sample of HDA is obtained. If HDA obtained from compression of LDA obtained by fast cooling (i.e., HGG) is then decompressed, this gives a new LDA sample different from the initial LDA (HGG).

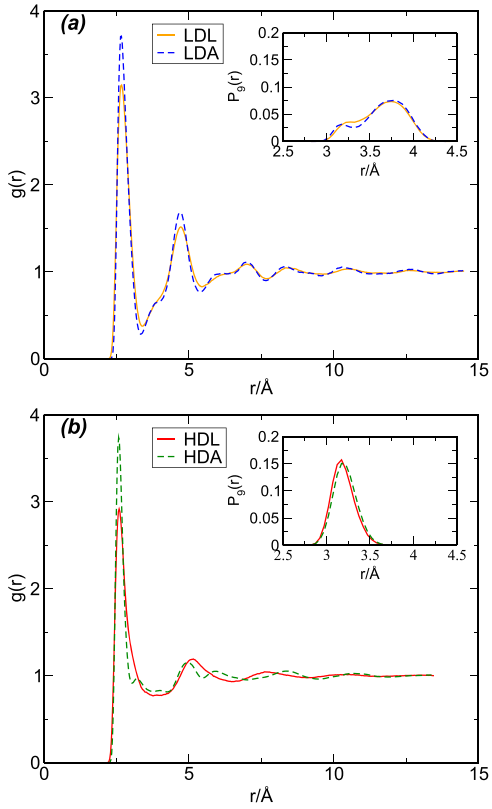

FIG. 1. (a) Radial distribution function of low-density liquid (LDL) at T = 420 K and low-density amorphous solid (LDA) at T = 200 K. (b) Radial distribution function of high density liquid (HDL) at T = 400 K and high-density amorphous solid (HDA) at T = 200 K. The insets show the probability distributions of ninth-nearest-neighbor distances of these configurations.

To examine the effects of the compression/decompression rate on PEL properties during the LDA–HDA transformation, we conduct a series of simulations with three different compression rates (5 MPa/ns, 10 MPa/ns, and 20 MPa/ns) along T = 200 K (see the supplementary material for q_{P1} and q_{P3}). We find that the qualitative behavior of the LDA–HDA transformation on the PEL is not significantly altered by increasing the compression rate from 5 MPa/ns to 20 MPa/ns. Therefore, we focus mainly on compression and decompression processes with q_{P2} = 10 MPa/ns.

We next explore the structural rearrangement of amorphous gallium upon compression and decompression along the paths from A to F and from G to L as shown in Fig. 2(a). As can be seen, P_{IS} changes linearly with volume, suggesting that the IS experiences an elastic deformation when the low-density HGG [point A in Fig. 2(a)] is compressed to 5 GPa (point D). Upon compression, the packing of gallium atoms becomes closer, indicated by the shift in the peaks of the RDF to lower values of r. Once P_{IS} goes beyond 5 GPa, the volume per particle jumps from v = 18 Å^3 to v = 17 Å^3, which is indicative of a discontinuous change. Correspondingly, a new peak in the RDF arises at $r \approx 2.3$ Å, accompanied by a broadening of the second peak at $r \approx 4.7$ Å [see Fig. 2(b)]. Meanwhile, two peaks in the distribution function of the ninth-nearest-neighbor merge into one [see the inset in Fig. 2(b)].

By comparing the structural features of LDA and HDA in Fig. 1, it is found that the discontinuous transformation upon compression [D to E in Fig. 2(a)] corresponds to a transformation from LDA to HDA. We note, however, that upon decompression from HDA [point G in Fig. 2(a)], no sharp change in $P_{IS}(v)$ is observed, even when the pressure is reduced to −3 GPa (point L) in metallic gallium. Since an LDA-like structure can be identified [Fig. 2(c)], this suggests a continuous transformation from HDA to an LDA-like structure upon decompression from G to L, which is different from what is found with the pairwise interaction models, such as the Jagla and Fermi–Jagla models,[34,35,45] for which a first-order-like transition can be recognized during decompression from HDA to LDA.

B. Comparison of the LDA–HDA and LDL–HDL transitions on the PEL

The question here concerns the nature of the LDA–HDA transformation in gallium, for instance, whether it is a first-order transition. We note that although equilibrium thermodynamics cannot be directly applied to out-of-equilibrium systems, its methods can be helpful in interpreting out-of-equilibrium behavior. For this, using the PEL method, we first explore the features of the equilibrium LDL–HDL first-order transition in configuration space, and we then study the signatures of the out-of-equilibrium LDA–HDA transformation upon compression and decompression on the PEL by comparing them with those of the equilibrium LLPT.

Figure 3 shows $P(v)$, $P_{IS}(v)$, $E_{IS}(v)$, and $S_{IS}(v)$ for different liquid isotherms (open symbols). For the liquids at T = 400 K and T = 420 K [see Figs. 3(a) and 3(e)], the $P(v)$ isotherms exhibit an Van der Waals loop around v = 20.3 Å^3 and 20.8 Å^3, respectively, a clear indication of phase separation into two liquid phases and consistent with the existence of a first-order LLPT of gallium as reported in Refs. 48 and 51.

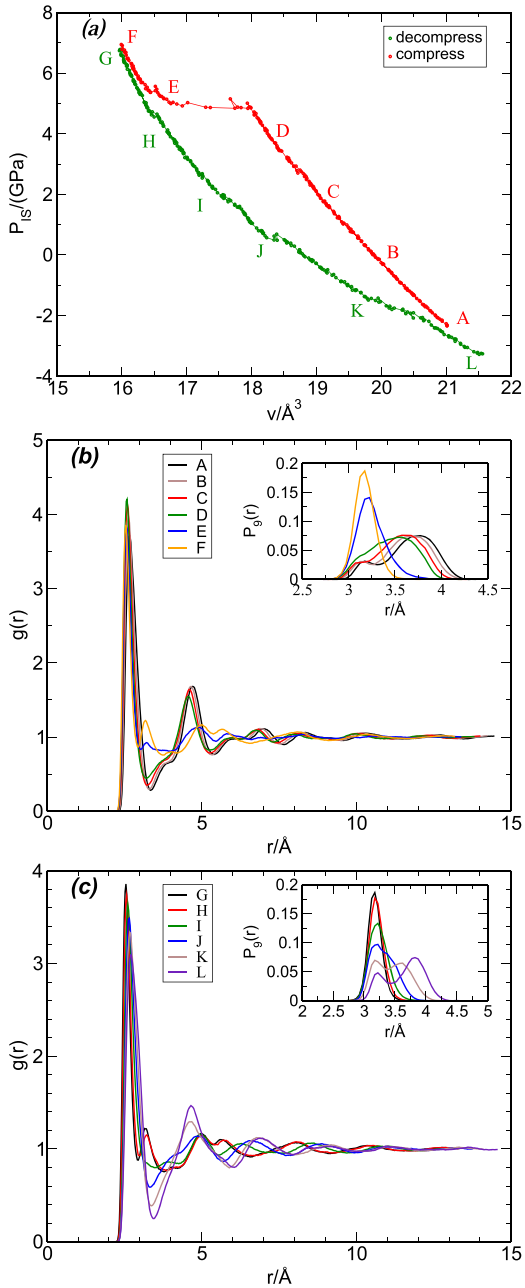

FIG. 2. (a) Inherent structure pressure P_{IS} as a function of volume along compression and decompression trajectories. (b) and (c) Radial distribution functions of glasses during compression and decompression, respectively. The insets in (b) and (c) show the probability distributions of ninth-nearest-neighbor distances.

From Figs. 3(b)–3(h), three characteristic features of the LLPT in PEL can be observed:

(i) $P_{IS}(v)$ exhibits a loop analogous to a van der Waals loop along the liquid isotherms.
(ii) $E_{IS}(v)$ shows a discontinuous change and a negative curvature.

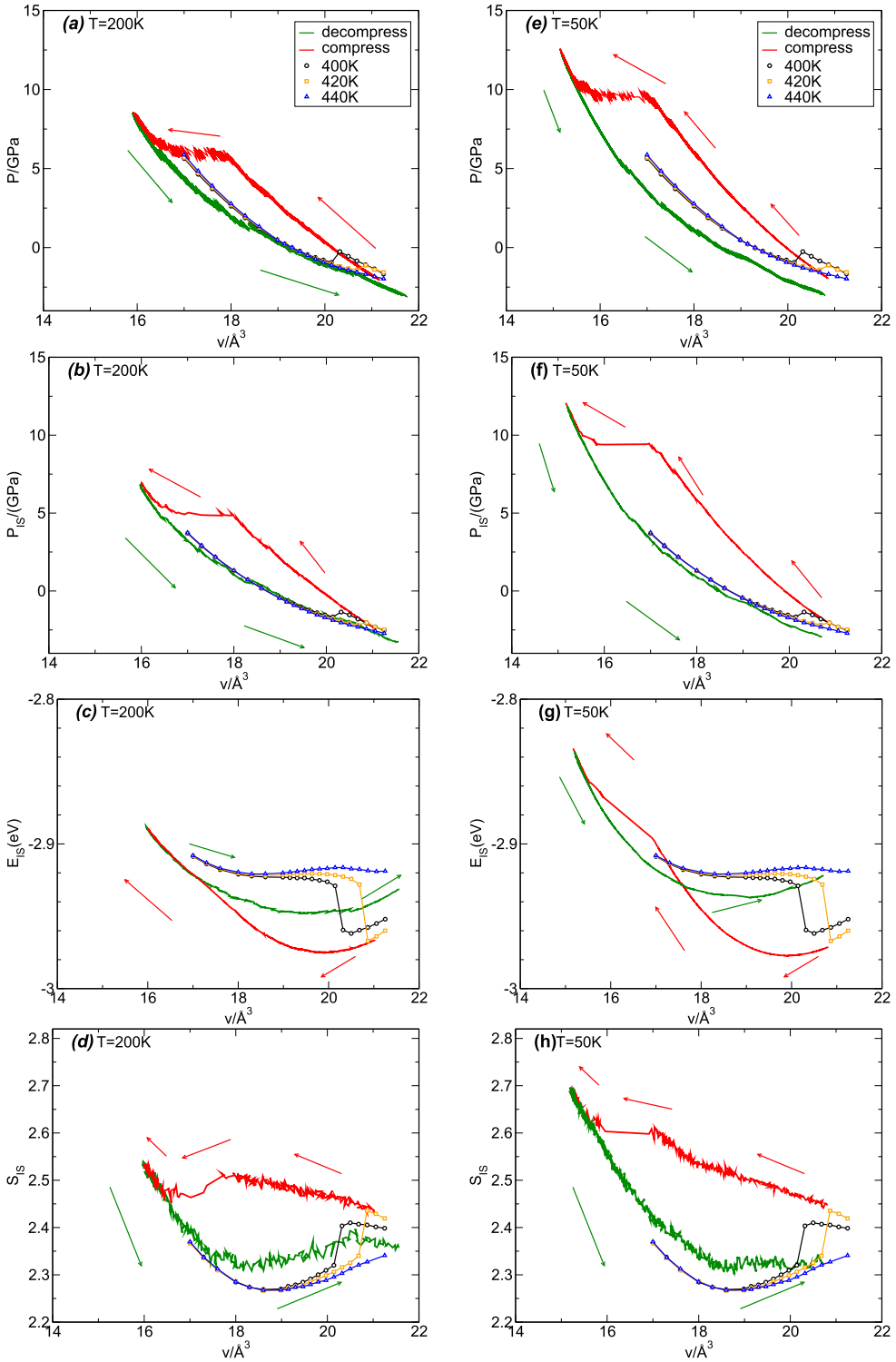

FIG. 3. (a) and (e) Pressure as a function of volume for gallium in liquid and glassy states upon compression/decompression. (b) and (f) IS pressure, (c) and (g) IS energy, and (d) and (h) IS shape function as functions of volume sampled during LLPT and one compression/decompression (red lines/green lines) cycle along T = 200 K and 50 K. Upon compression, the sharp change around P_{IS} = 5 GPa–6 GPa at 200 K and 9 GPa at 50 K indicates the existence of an LDA–HDA transformation. Black circles, orange squares, and blue triangles denote the liquid in equilibrium at 400 K, 420 K, and 440 K, respectively.

(iii) The shape function $S_{IS}(v)$ shows a sharp jump and a negative curvature from LDL to HDL.

We note that features (i) and (iii) here are the same as those of ST2 water,[30] but the discontinuity in $E_{IS}(v)$ for gallium is different from the behavior of ST2 water and the Fermi–Jagla model,[35] for both of which E_{IS} is continuous and has negative curvature. According to the analysis of the PEL properties of E_{IS} and S_{IS} during a first-order phase transition in Sec. II, the van der Waals loop in $P_{IS}(v)$ and the negative curvatures of $E_{IS}(v)$ and $S_{IS}(v)$ are responsible for the LLPT. Specifically, during the transformation of LLPT, P_{IS} exhibits a positive slope, $\partial P_{IS}/\partial V > 0$ (20 Å^3 < v < 21 Å^3) and E_{IS} exhibits a pronounced negative curvature $\partial^2 E_{IS}/\partial V^2 > 0$, so it violates the thermodynamic stable condition Eq. (4).

To characterize the PEL properties of the LDA–HDA transformation, we carry out five independent compression and decompression trajectories along T = 200 K and T = 50 K (prepared with the same cooling rate). We find that the qualitative behavior of the LDA–HDA transformation on the PEL does not significantly differ in these independent simulations. Therefore, for clarity, we present one compression and decompression process here (see the supplementary material for the five independent simulations). The pressure P, IS pressure P_{IS}, IS energy E_{IS}, and IS shape function S_{IS} are shown as functions of volume per particle in Fig. 3.

Similar to that of a liquid state, the pressure of a glassy state is a nonmonotonic function of volume. For instance, there exist clear plateaus at v = 17.5 Å^3 along T = 200 K [Fig. 3(a)] and at v = 16.5 Å^3 along T = 50 K [Fig. 3(e)], indicative of the existence of two amorphous states under the same pressure condition. Since $P_{vib} \propto T$ (constant V), at low temperatures, a van der Waals loop in P implies a van der Waals loop in P_{IS} in Figs. 3(b) and 3(f). Moreover, the P_{IS} curves of LDA and HDA overlap well with those of LDL and HDL, respectively. However, in terms of the IS energy E_{IS} [Figs. 3(c) and 3(g)], the LDA–HDA transformation differs from the LLPT. A negative curvature in E_{IS} develops along T = 50 K, but no abrupt change in E_{IS} is observed upon compression of LDA along T = 200 K and T = 50 K. This negative curvature in E_{IS}, consistent with the results of the ST2 model[30] and the Fermi–Jagla model,[35] is commonly considered as the signature separating the LDA and HDA megabasins on the PEL.

The shape function S_{IS} is another quantity describing how the system evolves on the PEL during the phase transformation. S_{IS} as a function of v during the LDL–HDL and LDA–HDA transitions is shown in Figs. 3(d) and 3(h). As can be seen, in each single pure phase (e.g., LDL/LDA or HDL/HDA), S_{IS} behaves monotonically on the PEL, mainly owing to the elastic transformation. S_{IS} becomes a nonmonotonic function of volume during phase transformations. For the LLPT, S_{IS} exhibits a discontinuous change as the volume varies, whereas for the LDA–HDA transformation, S_{IS} develops a negative curvature ($\partial^2 S_{IS}/\partial V^2 < 0$) at volumes v = 16 Å^3–17 Å^3 and v = 16.5 Å^3–17.5 Å^3 along T = 50 K and T = 200 K, respectively. This characteristic is also found in the ST2 water model.[30]

In brief, the LDA–HDA transformation exhibits three main features on the PEL:

(a) van der Waals-like loops in $P_{IS}(v)$,
(b) negative curvature in $E_{IS}(v)$ at low T, and
(c) negative curvature of $S_{IS}(v)$ as a function of volume.

All three characteristics are consistent with features (i)–(iii) of an LLPT, and hence, the out-of-equilibrium transformation between LDA and HDA in gallium can be identified as a first-order-like phase transition. Meanwhile, these three main PEL features during the LDA–HDA transformation are also consistent with what has been found in previous studies.[30,35]

C. Transformation path of the LDA–HDA transition on the PEL

In this subsection, we compare the transformation path of amorphous samples with that of equilibrium liquid samples on the PEL for gallium. As can be seen from Fig. 4, the initial LDA (HGG) configurations (black empty squares) are very close to the LDL equilibrium liquid states (solid black squares) at the same densities, but the glassy states explored on the PEL upon compression/decompression start to deviate from the accessible configuration region explored by equilibrium liquids. For example, even at the

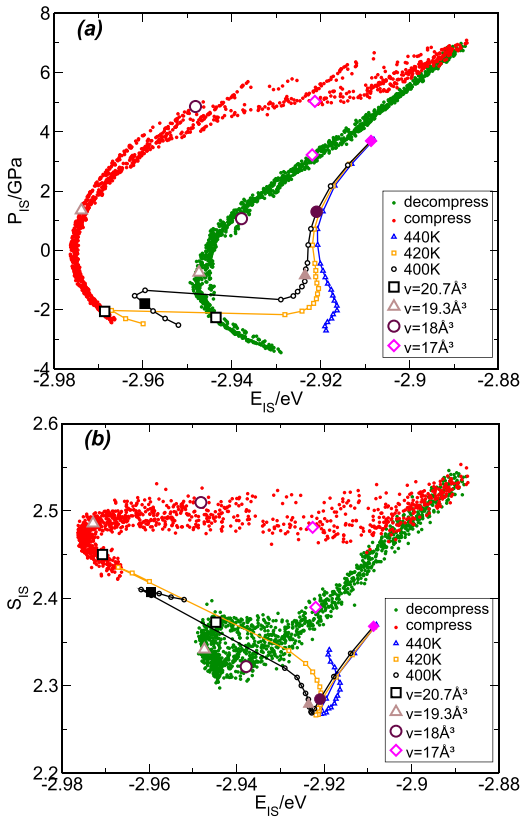

FIG. 4. (a) P_{IS} and (b) S_{IS} as functions of E_{IS} upon compression/decompression along T = 200 K. Red and green dots represent the five independent compression and decompression processes, respectively. Black circles, orange squares, and blue triangles correspond to IS properties of the equilibrium liquid along 400 K, 420 K, and 440 K, respectively. Black squares, brown triangles, indigo circles, and magenta diamonds are configurations for v = 20.68 Å^3, 19.30 Å^3, 18.00 Å^3, and 17.00 Å^3, respectively. The same symbols (black squares, brown triangles, indigo circles, and magenta diamonds) represent systems with the same density, with empty symbols representing amorphous solids and solid symbols representing liquids.

same density, the HDA and HDL are widely separated on the (E_{IS}, P_{IS}) plane and the (S_{IS}, E_{IS}) plane. The LDA-like state (green dots in Fig. 4) obtained by decompression from HDA is also not accessible for liquids. Moreover, the LDA–HDA trajectories on the PEL induced by both compression (red dots) and decompression (green dots) cannot be matched to the LDL–HDL trajectories at all. This suggests that the LDA–HDA transformations occur in the region of the PEL where the LLPT cannot explore. The paths of the LDA and HDA transformations on the PEL are also inaccessible to the LLPT. We stress that even the amorphous states are strongly dependent on how they are prepared, with regard to, for example, cooling rates and compression/decompression rates, the amorphous solids (LDA and HDA) cannot be considered simply as the "frozen" configurations of the corresponding equilibrium liquids (LDL and HDL) on the PEL. This result that we find in gallium is in agreement with those of previous simulations of water using the ST2 and SPC/E models and FJ liquid.[30,31,35]

IV. DISCUSSION AND SUMMARY

Gallium is among the substances that exhibit a series of anomalies and an LLPT and LLCP. Specifically, it is a metallic system with many-body interactions and thus differs from model systems based on pairwise potentials, such as various water models and the Jagla and Fermi–Jagla models. Therefore, investigation of the out-of-equilibrium amorphous–amorphous transition (LDA–HDA) of gallium and its relationship with the equilibrium LDL–HDL transition is significant for providing a deeper understanding of nonequilibrium phase transformations. From the results obtained here, both similarities and differences in PEL properties have been found in the LDA–HDA transition of gallium compared with substances with pairwise interactions.

Upon compression, a van der Waals-like loop in $P_{IS}(v)$ of gallium is observed in Figs. 3(b) and 3(f), suggesting the possible existence of two glassy phases on the PEL. This feature of $P_{IS}(V)$ is also found in ST2 water[30] and the Fermi–Jagla model.[35] In the case of ST2 water, $E_{IS}(v)$ develops a maximum on the PEL during the LDA–HDA transformation, indicative of the existence of two megabasins on the PEL.[30] By contrast, in the case of gallium, $E_{IS}(v)$ develops a negative curvature upon compression at low temperature (e.g., T = 50 K), but not at high temperature (e.g., T = 200 K), which is consistent with a recent study indicating that it is the curvature change in $E_{IS}(v)$ that establishes the boundary between two megabasins.[35] This phenomenon is in agreement with what is found for SPC/E water, namely, that concavity in $E_{IS}(v)$ is apparent at a temperature close to 0 K but is rather weak at 77 K.[31] For the 4 substances discussed above (FJ, ST2, gallium and SPC/E), we think that the differences in the features of the PEL properties, P_{IS} and E_{IS}, may be due to the differences in the stability of their LLCPs. In the case of substances with accessible LLCP (FJ, ST2 and gallium), during the LDA-HDA transformation (i) P_{IS} exhibits van der Waals-like loops, (2) E_{IS} exhibits negative curvatures. However, for the case of substance without accessible LLCP (SPC/E), at finite temperatures, there are no clear van der Waals-like loops for PIS and negative curvatures for E_{IS}. Interestingly, a negative curvature of the shape function $S_{IS}(v)$ of the basins is observed in gallium. Specifically, S_{IS} exhibits $\partial^2 S_{IS}/\partial V^2 < 0$ at v = 16 Å^3–17 Å^3 and at v = 16.5 Å^3–17.5 Å^3 along T = 50 K and T = 200 K, respectively. Similar features are also observed in ST2 water. However, for the Fermi–Jagla model, the shape function S_{IS} is a monotonic function of volume, which means that the basins become thinner smoothly during the LDA–HDA transformation on compression. Non-monotonic behavior in SIS is also weak in SPC/E during compression and absent during decompression. In addition, we do not find any van der Waals-like loops in $P_{IS}(v)$ or any negative curvatures of S_{IS} upon decompression in gallium, in contrast to the PEL behavior of ST2 water[30] and the Fermi–Jagla model.[35] This means that for gallium, the path that the glassy system follows on the PEL upon decompression is different from that upon compression.

To summarize, we have investigated the signatures of the LDA–HDA transition of gallium in the PEL formalism and have compared them with those of the LLPT. We have found that by rapid cooling or compression/decompression, two distinct amorphous solid phases of gallium, namely, LDA and HDA, can be obtained, where LDA of gallium shares similar structures with an LDL, while HDA shares similar structures with an HDL. The LDA–HDA transformation occurs in the region that liquids cannot explore on the PEL. The signatures of this out-of-equilibrium transition are reminiscent of those of the equilibrium LLPT on the PEL, such as a van der Waals-like loop in the IS pressure, a negative curvature of the IS energy separating two megabasins (LDA/LDL and HDL/HDA), and nonmonotonic behavior of the shape function. This suggests that the LDA–HDA transformation is first-order-like and provides significant information for the study of amorphous–amorphous transitions in metallic systems with many-body interactions, which is crucial for further understanding of the nature of the polyamorphic family.

SUPPLEMENTARY MATERIAL

In the supplementary material, all five independent results obtained for glassy gallium with compression rate q_2 = 10 MPa/ns at 50 K and 200 K are included. The results obtained for glassy gallium with compression rates q_1 = 5 MPa/ns and q_3 = 20 MPa/ns are also included.

ACKNOWLEDGMENTS

We thank Dr. Nicolas Giovambattista for helpful discussions. Y.L. and L.X. acknowledge the National Natural Science Foundation of China (Grant Nos. 11935002 and 11525520), the National Basic Research Program of China (973 Program, Grant No. 2015 CB856801), and the National Key Research and Development Program of China (Grant No. 2016Y FA0300901). We are grateful for the computational resources provided by TianHe-1A and the High-Performance Computing Platform of Peking University.

DATA AVAILABILITY

The data that support the findings of this study are available from the corresponding authors upon reasonable request.

REFERENCES

[1] R. J. Speedy and C. A. Angell, J. Chem. Phys. **65**, 851–858 (1976).
[2] C. A. Angell, J. Shuppert, and J. C. Tucker, J. Chem. Phys. **77**, 3092–3099 (1973).

[3]C. A. Angell, Annu. Rev. Phys. Chem. **34**, 593–630 (1983).
[4]S. Sastry and C. Austen Angell, Nat. Mater. **2**, 739–743 (2003).
[5]A. Cadien, Q. Y. Hu, Y. Meng, Y. Q. Cheng, M. W. Chen, J. F. Shu, H. K. Mao, and H. W. Sheng, Phys. Rev. Lett. **110**, 125503 (2013).
[6]P. H. Poole, F. Sciortino, U. Essmann, and H. E. Stanley, Nature **360**, 324 (1992).
[7]P. G. Debenedetti and H. E. Stanley, Phys. Today **56**(6), 40 (2003).
[8]C. A. Angell, Annu. Rev. Phys. Chem. **55**, 559–583 (2004).
[9]P. H. Poole, F. Sciortino, U. Essmann, and H. E. Stanley, Phys. Rev. E **48**, 3799–3817 (1998).
[10]L. Xu, P. Kumar, S. V. Buldyrev, S.-H. Chen, P. H. Poole, F. Sciortino, and H. E. Stanley, Proc. Natl. Acad. Sci. U. S. A. **102**, 16558–16562 (2005).
[11]L. Xu, F. Mallamace, Z. Yan, F. W. Starr, S. V. Buldyrev, and H. Eugene Stanley, Nat. Phys. **5**, 565–569 (2009).
[12]Y. Duan, T. Li, W. Wu, J. Li, X. Zhou, S. Liu, and H. Li, Chin. Phys. B **26**, 036401 (2016).
[13]C. Yang, C. Zhang, F. Ye, and X. Zhou, Chin. Phys. B **28**, 116104 (2019).
[14]Z. Sun, G. Sun, Y. Chen, and L. Xu, Sci. Chin. Phys. Mech. Astron. **57**, 810–818 (2014).
[15]Y. Katayama, T. Mizutani, W. Utsumi, O. Shimomura, M. Yamakata, and K.-i. Funakoshi, Nature **403**, 170–173 (2000).
[16]L. I. Aptekar, Sov. Phys. Dokl. **24**, 993–995 (1979).
[17]V. V. Vasisht, S. Saw, and S. Sastry, Nat. Phys. **7**, 549–553 (2011).
[18]P. Ganesh and M. Widom, Phys. Rev. Lett. **102**, 075701 (2009).
[19]N. Jakse and A. Pasturel, Phys. Rev. Lett. **99**, 205702 (2007).
[20]M. Beye, F. Sorgenfrei, W. F. Schlotter, W. Wurth, and A. Föhlich, Proc. Natl. Acad. Sci. U. S. A. **107**, 16772–16776 (2000).
[21]I. Saika-Voivod, F. Sciortino, and P. H. Poole, Phys. Rev. E **63**, 011202 (2000).
[22]R. J. Speedy, J. Phys. Chem. **86**, 982–991 (1982).
[23]P. H. Poole, F. Sciortino, T. Grande, H. E. Stanley, and C. A. Angell, Phys. Rev. Lett. **73**, 1632 (1994).
[24]S. Sastry, P. G. Debenedetti, F. Sciortino, and H. E. Stanley, Phys. Rev. E **53**, 6144 (1996).
[25]C. A. Angell, Science **319**, 582–587 (2008).
[26]P. Chitnelawong, F. Sciortino, and P. H. Poole, J. Chem. Phys. **150**, 234502 (2019).
[27]O. Mishima, L. D. Calvert, and E. Whalley, Nature **310**, 393–395 (1984).
[28]O. Mishima, L. D. Calvert, and E. Whalley, Nature **314**, 76–78 (1985).
[29]K. H. Kim *et al.*, Science **370**, 978–982 (2020).
[30]N. Giovambattista, F. Sciortino, F. W. Starr, and P. H. Poole, J. Chem. Phys. **145**, 224501 (2016).
[31]N. Giovambattista, H. E. Stanley, and F. Sciortino, Phys. Rev. Lett. **91**, 115504 (2003).
[32]N. Giovambattista, T. Loerting, B. R. Lukanov, and F. W. Starr, Sci. Rep. **2**, 390 (2012).
[33]N. Giovambattista, F. W. Starr, and P. H. Poole, J. Chem. Phys. **147**, 044501 (2017).
[34]L. Xu, N. Giovambattista, S. V. Buldyrev, P. G. Debenedetti, and H. E. Stanley, J. Chem. Phys. **134**, 064507 (2011).
[35]G. Sun, L. Xu, and N. Giovambattista, Phys. Rev. Lett. **120**, 035701 (2018).
[36]J. Wong, D. A. Jahn, and N. Giovambattista, J. Chem. Phys. **143**, 074501 (2015).
[37]P. H. Handle, F. Sciortino, and N. Giovambattista, J. Chem. Phys. **150**, 244506 (2019).
[38]N. Giovambattista, F. W. Starr, and P. H. Poole, J. Chem. Phys. **150**, 244502 (2019).
[39]O. Mishima, J. Chem. Phys. **100**, 5910 (1994).
[40]E. L. Gromnitskaya, O. V. Stal'gorova, V. V. Brazhkin, and A. G. Lyapin, Phys. Rev. B **64**, 094205 (2001).
[41]S. Klotz, T. Strassle, R. J. Nelmes, J. S. Loveday, G. Hamel, G. Rousse, B. Canny, J. C. Chervin, and A. M. Saitta, Phys. Rev. Lett. **94**, 025506 (2005).
[42]M. M. Koza, B. Geil, K. Winkel, C. Kohler, F. Czeschka, M. Scheuermann, H. Schober, and T. Hansen, Phys. Rev. Lett. **94**, 125506 (2005).
[43]K. Winkel, M. S. Elsaesser, E. Mayer, and T. Loerting, J. Chem. Phys. **128**, 044510 (2008).
[44]P. H. Handle and T. Loerting, J. Chem. Phys. **148**, 124508 (2018).
[45]J. Y. Abraham, S. V. Buldyrev, and N. Giovambattista, J. Phys. Chem. B **115**, 14229–14239 (2011).
[46]B. D. Sharma and J. Donohue, Z. Kristallogr. **117**, 293–300 (1962).
[47]L. Bosio, J. Phys. Chem. **68**, 1221 (1978).
[48]R. Li, G. Sun, and L. Xu, J. Chem. Phys. **145**, 054506 (2016).
[49]M. I. Baskes, Phys. Rev. B **46**, 2727–2742 (1992).
[50]M. I. Baskes, S. P. Chen, and F. J. Cherne, Phys. Rev. B **66**, 104107 (2002).
[51]D. A. C. Jara, M. F. Michelon, A. Antonelli, and M. de Koning, J. Chem. Phys. **130**, 221101 (2009).
[52]F. H. Stilinger, Science **267**, 1935 (1995).
[53]F. Sciortino, J. Stat. Mech. **2005**, P05015.
[54]S. Sastry, Nature **409**, 164 (2001).
[55]J. P. Perdew, Physica B **172**, 1 (1991).
[56]S. Plimpton, J. Comput. Phys. **117**, 1 (1995).
[57]G. Sun, L. Xu, and N. Giovambattista, J. Chem. Phys. **146**, 014503 (2017).
[58]P. G. Debenedetti and F. H. Stillinger, Nature **410**, 259 (2001).
[59]T. M. Nymand and P. Linse, J. Chem. Phys. **112**, 6152 (2000).